Improving Wind Speed Availability of a Six-Beam Doppler Lidar

Mohammadreza Manami[1, 2], Guillaume Léa[2], Jakob Mann[1], Mikael Sjöholm[1], and Guillaume Gorju[2]

[1]DTU Wind and Energy Systems, Technical University of Denmark, Roskilde, Denmark
[2]Lidar Division, Lumibird SA, Lannion, France

Correspondence: Mohammadreza Manami (manami@dtu.dk)

Abstract. A simple adaptive variant of the Doppler beam swinging method is presented to enhance the availability of wind velocity measurements in profiling lidars. The adaptive method dynamically selects Doppler velocities from beams that have sufficient signal-to-noise ratios in their backscattered signals. Then it uses those Doppler velocities for wind velocity reconstruction, rather than relying on the standard approach which discards the entire scan whenever even one beam's backscattered signal does not meet the signal-to-noise requirement. The adaptive method was validated in two measurement campaigns at the Østerild wind turbine test field in Denmark using three BEAM 6x profiling lidars from Lumibird. In the first campaign, a lidar measured up to 500 m in proximity to a meteorological mast; in the second campaign, the first lidar was replaced by two other lidar units to increase the maximum measurement range up to 1 km. Validation against cup anemometers and wind vanes at four different heights of the met mast showed excellent agreement for mean wind speed and wind direction, with results similar to those from the standard approach. Availability assessments indicated improvements for all three lidars at high altitudes, showing a maximum increment of 16.9 percentage points over the standard approach. Due to its simplicity, the adaptive method can be implemented in lidar software without requiring any hardware modifications.

1 Introduction

As modern wind turbines are increasingly deployed at heights spanning the entire atmospheric boundary layer (ABL), understanding the physics of the entire ABL has become more essential (van Kuik et al., 2016; Veers et al., 2019, 2023). In recent years, wind Doppler lidars have emerged as a popular and cost-effective alternative to meteorological masts, offering the capability to measure wind profiles at significantly greater heights. However, one of the challenges in extended ranges of profiling lidars is the weakening of atmospheric backscatter signals, due to beam divergence and aerosol-related attenuation of the laser beam (Ceolato and Berg, 2021; Measures, 1984). The aim of this study is to introduce a simple algorithm that increases the instantaneous availability of reconstructed wind velocities by adaptively selecting the maximum number of beams with an adequate signal-to-noise ratio (SNR) in their backscattered signals.

Doppler beam swinging (DBS) is a well-established and widely used method for reconstructing wind velocities from Doppler velocity measurements (Lehmann and Brown, 2021; van Dooren, 2022). DBS requires at least three Doppler velocities from non-coplanar beams to reconstruct the three components of the wind vector. Most commercial pulsed profiling lidars use more than three beams to improve the accuracy of this reconstruction. In this study, we propose an adaptive algorithm for selecting among the six beams of the Lumibird profiling lidar, aimed at improving the availability of reconstructed wind

velocities, particularly at higher altitudes. The current standard DBS setup on this instrument rejects an entire scan of six Doppler velocities if any of the backscattered signal intensities from inclined beams fall below the factory-set SNR threshold. This limitation becomes evident at higher altitudes, where the backscattered signal from some beams no longer meets the SNR requirement, resulting in a loss of usable Doppler velocities from other beams. Our adaptive approach mitigates this issue by selectively using only those beams that satisfy the SNR requirement for backscattered signals, thereby maintaining reliable wind velocity retrievals while increasing data availability. Despite the variety of scanning patterns and suggested elevation and azimuth angles for wind lidars (Steinheuer et al., 2022), this study focuses on a fixed beam geometry due to hardware limitations. Nevertheless, a similar algorithm could be applied to instruments operating on the same principle. The work presented here offers several aspects compared to previous studies that reveal interesting insights and diverse perspectives. One aspect is that the validation of measurements is performed at higher altitudes, up to 244 m, where reduced availability makes accuracy assessment more demanding compared to lower altitudes (e.g., 90 m), where availability is nearly complete and accuracy is generally assured. Extending this validation to even higher altitudes would be especially valuable, as the differences between the accuracy of DBS methods are expected to become more pronounced as variations in availability are more significant. The adaptive method provides an additional advantage in terms of the beam blockage issue. If one beam is blocked by a solid object or otherwise compromised, velocities can still be retrieved using a combination of the remaining beams. This addresses a common issue faced by clients, who sometimes must return complete datasets to lidar manufacturers for post-processing of the Doppler measurements when a single inclined beam is blocked or otherwise compromised, as no velocity reconstruction is possible in the current setup under these conditions. Using the adaptive algorithm, this problem is avoided, allowing the retrieval of velocity without the manufacturer's intervention, and also saving significant time and effort.

2 Methodology

The DBS technique in pulsed lidar is conceptually adopted from the velocity azimuth display (VAD) method, which was originally developed for use in radar systems (Lhermitte, 1961; Browning and Wexler, 1968). Both the VAD and DBS techniques involve measuring mean Doppler velocities at positions that form a cone above the instrument which is placed in the apex. In the VAD technique, the lidar beam rotates continuously at a fixed elevation angle, while the DBS approach typically relies on a discrete set of static beams. Under the assumption of a horizontally homogeneous and steady wind field at a given height, the complete wind vector can be retrieved by minimizing the squared differences between the measured radial velocities and the corresponding projections of the wind vector onto the unit vectors aligned with each beam.

$$\chi^2 = \sum_{i=1}^{N} \frac{(\boldsymbol{u} \cdot \boldsymbol{r}_i - u_{ri})^2}{\sigma_{ri}^2}, \tag{1}$$

In the above equation, $\boldsymbol{u} = (u, v, w)$ denotes the mean wind velocity vector to be determined, N is the number of lidar beams, u_{ri} is the radial velocity measured along the i-th beam, and σ_{ri} represents its associated uncertainty (Newsom et al., 2017). The unit vector $\boldsymbol{r}_i$, which defines the orientation of each lidar beam, is given by:

$$\boldsymbol{r}_i = (\cos\alpha_i \cos\theta_i, \cos\alpha_i \sin\theta_i, \sin\alpha_i), \tag{2}$$

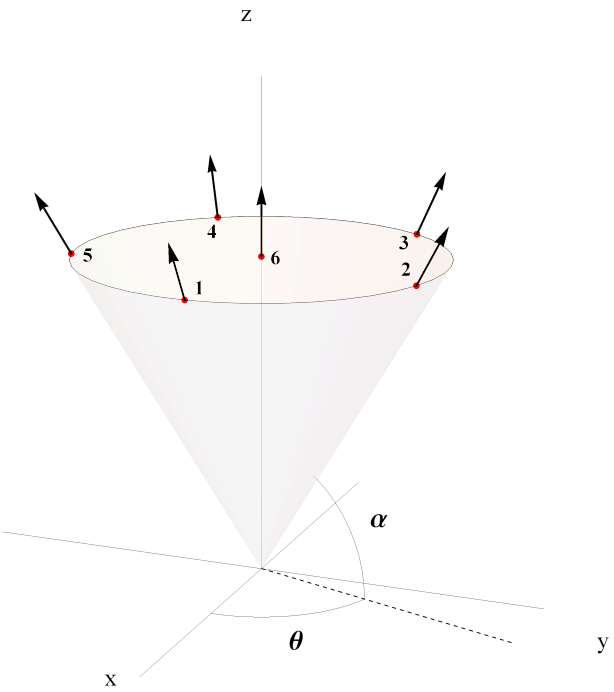

Figure 1. Beam directions for BEAM 6x Lumibird lidar. The instrument has five inclined beams at approximately 60° elevation, evenly spaced every 72° in azimuth from 0° to 360° (numbers 1 to 5, respectively), along with a vertical beam at 90° elevation (number 6).

where α_i and θ_i are the elevation and azimuth angles, respectively. The BEAM 6x Lumibird lidar includes five beams with elevation angles near 60 degrees, distributed evenly in azimuth with 72-degree spacing on the full 360-degree circle (see Figure 2). It also features a single vertical beam with a 90-degree elevation. The beams are numbered from 1 to 6, where beams 1 through 5 represent the inclined beams arranged in increasing azimuth angles starting from zero degrees, and beam 6 corresponds to the vertical beam. The BEAM 6x lidar system operates with a pulse width of 150 ns, a laser power of 20 μJ, and a pulse repetition frequency of 10 kHz, while its acquisition board samples data at 50 MHz. This system performs a complete scan every 5.5 seconds, providing Doppler velocities every 3 m along the beams.

In the standard DBS setup on the BEAM 6x, DBS requires valid measurements of all radial velocities from the inclined beams at the target height; otherwise, the entire scan is rejected. This study proposes a simple method that applies DBS using the maximum number of beams, which is particularly useful when the backscattered signal from some beams fails to meet the SNR threshold.

The procedure of the proposed adaptive DBS is presented in Figure 2. The algorithm begins by applying a sliding time window to Doppler velocities. At each height, the window contains six consecutive Doppler velocity measurements, one from each of the six beams. First, the algorithm filters out any radial velocities with an SNR below a predefined factory threshold. If at least three valid Doppler velocities remain, a DBS process is performed. Before applying the DBS method, a quality check

is adopted to verify the reliability of the estimated wind components. This step is designed to identify so-called ill-conditioned scenarios, which occur when only three beams are available and their azimuthal orientations are poorly distributed, typically when the line-of-sight vectors lie nearly in one plane. This algorithm effectively excludes only five sets of three-beam, which correspond to the least accurate cases among the 42 possible combinations (not shown here). The five excluded combinations are 1-3-6, 1-4-6, 2-4-6, 2-5-6, and 3-5-6 (see Figure 1), as they are considered to be ill-conditioned scenarios. This algorithm continues until either a valid solution is found or fewer than three beams remain, at which point a solution is no longer feasible. In this algorithm, the objective is to increase instantaneous availability. A comparison with fixed configurations will logically show that wind speed availability will always be equal to or higher for the adaptive method, as a fixed configuration is merely a subset when the SNR constraint is satisfied.

Another criterion that can be discussed is the residuals of the fit to Doppler velocities (Steinheuer et al., 2022), which can be calculated after performing DBS. We do not recommend relying on this metric, as high turbulence can also result in a high residual, making it difficult to differentiate between a poor fit and turbulent flow.

Availability A is defined as the ratio of filtered instantaneous reconstructed velocities N_f to the total number of complete scans N_t. For the adaptive method, N_f corresponds to the number of reconstructed wind velocities remaining after applying all the filters shown in Figure 2. In the standard method, N_f refers to the number of reconstructed wind velocities from the five inclined beams after the intensity filter is applied.

$$A = \frac{N_f}{N_t} \times 100 \tag{3}$$

The proposed adaptive DBS approach was evaluated through field experiments using three BEAM 6x profiling lidars during two measurement campaigns at the Østerild wind turbine test field (Peña, 2019). Ten-minute mean wind speeds and wind directions obtained from the lidars with adaptive DBS were compared against reference measurements from cup anemometers and wind vanes installed on a nearby meteorological mast. Also, results from the standard DBS method are included. The following filters were applied to both standard DBS and adaptive methods to ensure the validity of the comparison with reference instruments, which is also aligned with the DTU calibration report (Hansen and Yankova, 2024).

- Lidar Data Availability: Only 10-minute intervals containing at least 75% of the total possible complete scans were included in the analysis to ensure the reliability and representativeness of the mean wind speeds and wind directions.
- Wake-Free Sector: Wind directions from the westerly sector (195° to 355°) were selected to avoid interference from a nearby wind turbine and meteorological mast. This sector is broader than the range of 240° to 300° recommended in the DTU calibration report, in order to provide more 10-minute average data points for the validation of adaptive DBS.
- Wind Speed Range: The analysis was limited to 10-minute average wind speeds between 4 m/s and 16 m/s, consistent with the valid operating range of standard cup anemometers as defined by the IEC standard (IEC, 2022).

The DTU calibration report (Hansen and Yankova, 2024) implements an additional filtering criterion to remove the effects of potential icing, specifically excluding wind speeds collected at temperatures below 2°C. This temperature-based filter was

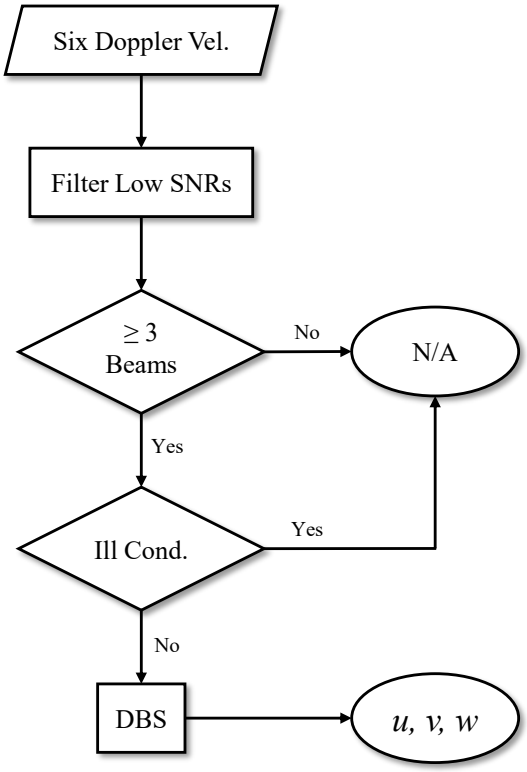

Figure 2. Algorithm of adaptive DBS.

not applied in our analysis, as it only affected a small portion of the measurements. To validate and certify the estimated mean wind speeds and wind directions, the linear regression slope and the coefficient of determination R^2, between the lidar measurements and the reference instruments should typically fall within the acceptable range of 0.98 to 1.02. In this work, the proposed method was validated at four heights ranging from 40 m to 244 m, after which data availability was examined for heights up to 980 m.

3 Field Experiment

The field experiment was conducted at the Danish National Test Station for Large Wind Turbines in Østerild, Northern Jutland, Denmark. Three BEAM 6x Wind Sciences (HALO Photonics by Lumibird, 2024) profiling lidars were installed west of the Light Mast North over two separate deployment periods. The profiling lidars are hereafter identified by the last three digits of their serial numbers: 205, 320, and 325. The first campaign, using BEAM 6x-205, took place from October 13, 2023, to January

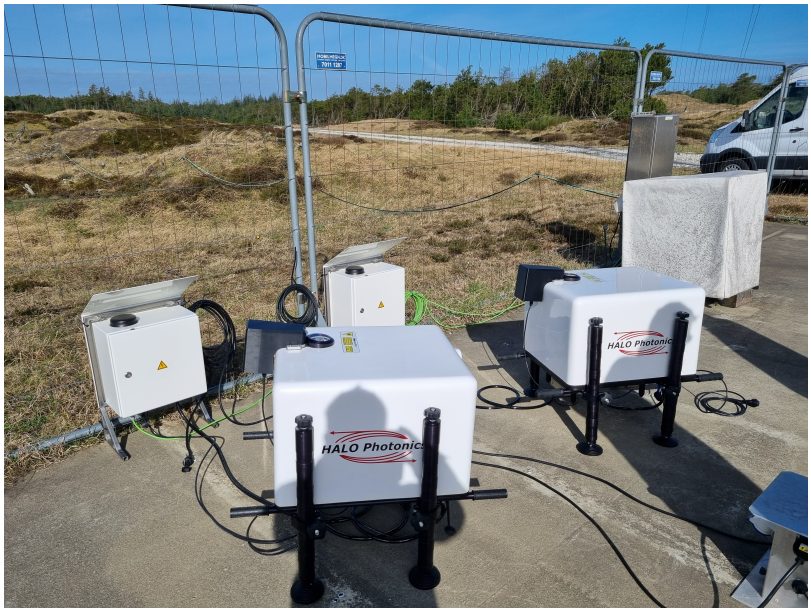

Figure 3. Two BEAM 6x profiling lidars manufactured by Lumibird during installation at the Østerild test site.

9, 2024, during which wind profiles were measured up to 500 m. Subsequently, lidar units 320 and 325 were installed in the same place, from October 3 and November 13, respectively, extending the measurement range up to 1 km until December 6, 2024. All three lidar units operated independently, and the BEAM 6x system allows users to specify a maximum range that exceeds its 500-m design range. Figure 4 displays the installation site of BEAM 6x-205, where the two other units were later installed at approximately the same position. In the field experiment, Doppler velocities are collected from three lidars to implement adaptive DBS and to compare its availability with the standard DBS method.

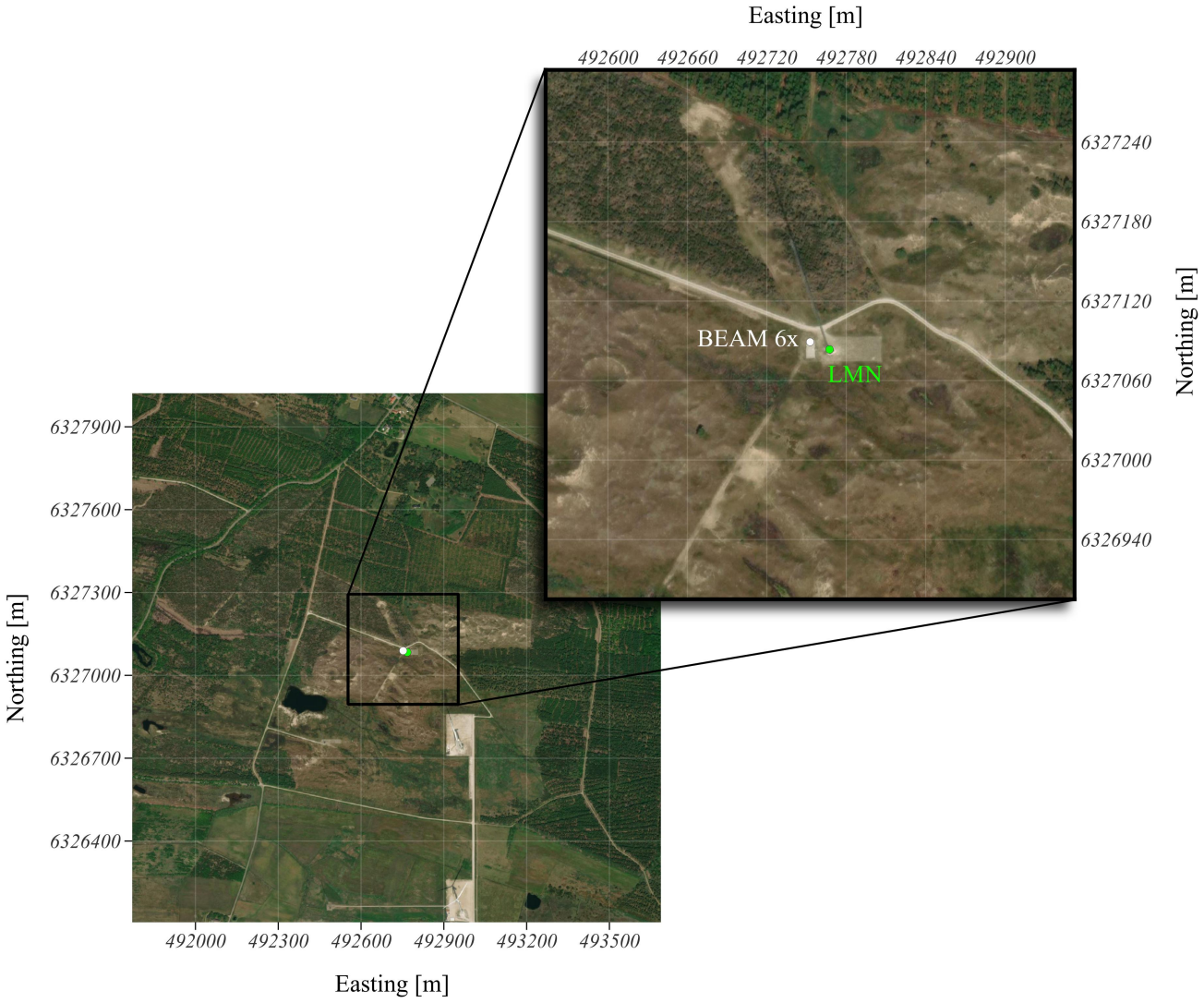

Figure 4. Satellite image of the experimental field at Østerild test site (Denmark) from Bing Maps, copyright 2025 © Microsoft. The BEAM 6x profiling lidar (white dot) with serial number 205 is located near the Light Mast North (green dot). Two other units were later installed at approximately the same location.

4 Results and Discussion

The adaptive DBS method was validated by comparing 10-minute averaged wind speeds and directions against reference measurements from cup anemometers and wind vanes, following the filtering procedure described in Section 2. Validation results are summarized in Tables 1, A1, and A2 for BEAM 6x-205, 320, and 325, respectively. For comparison, the results from the standard DBS, similar to the current implementation in BEAM 6x instruments, are also included.

The evaluation metrics include the slope of the Deming regression line constrained through the origin, the coefficient of determination R^2, and the root mean square error $RMSE$. In calibration reports, either ordinary least squares or orthogonal least squares regression is typically applied to both wind speed and wind direction. However, because wind direction is a circular variable, we recommend using angle versus angle fitting (see Appendix B), where a unity slope is assumed, and the circular offset is calculated. For completeness, we also report the Deming regression slope for wind direction. These metrics were computed at four selected heights: 40 m, 106 m, 178 m, and 244 m, because both reference cup anemometers and wind vanes are available at these levels.

The adaptive method demonstrates excellent agreement with the reference instruments for both wind speed and wind direction, and its performance closely matches that of the standard DBS method. At lower heights, data availability is similar for the two methods, but as height increases, the adaptive method provides greater availability. For instance, at 244 m in BEAM 6x-320, availability increases from 78.7% with the standard approach to 88.8% with the adaptive approach (Table A1).

Across all reference heights and among the three units, only BEAM 6x-320 at 40 m exhibited a slight degradation in wind direction $RMSE$, which is caused by a small number of outliers in the regression analysis. An additional enhancement to the adaptive DBS could involve implementing a spike filter that compares the Doppler velocity of each beam with its two temporal neighbors. The spike filter could help suppress weak velocity estimates while preserving a similar high availability. However, this filter was not included in the present analysis since this study is focused on the adaptive beam selection algorithm, and the combined effect of spike filtering and SNR thresholds is a big topic for investigation in itself. Also, spike detection for each beam requires access to the radial velocity measurement from the subsequent time step, which becomes available approximately five seconds later in BEAM 6x, once a scan is completed. As a result, implementing such an algorithm would introduce a slight delay of a few seconds relative to real-time measurements. In the adaptive DBS algorithm, the objective was to apply only minor modifications to the original BEAM 6x algorithm, especially without altering the factory-defined SNR threshold. While small adjustments to the SNR threshold could further improve availability, such changes would risk compromising velocity estimation accuracy. The original design specifications of the BEAM 6x lidar target wind profiling up to 500 m; therefore, some of the design parameters might need reconsideration when aiming for higher altitudes.

As an example of regression analysis, Figure 5 presents the 10-minute averaged wind speed and wind direction at a height of 244 m for BEAM 6x-205 against reference instruments, in order to compare results from the standard and adaptive DBS methods. The distribution of data points, regression lines, and derived statistical metrics is comparable between the two approaches, supporting the validity of the proposed adaptive DBS technique. As noted in Section 2, the DTU calibration report limits the analysis sector to 240°–300°. However, the present study considers a broader sector to increase the number of available 10-

minute data points. This broader inclusion may contain distortions from the Light Mast North guy wires located at 210° and 330°. In the wind direction regression plots, localized scatter appears near these angles, likely due to the distortion effect of the guy wires.

Table 1. Validation of DBS methods using Doppler velocities from BEAM 6x-205. Estimated wind speed (WS) and wind direction (WD) are compared with reference cup anemometer and wind vane measurements.

height [m]	method	A [%]	variable	Deming regression, slope [-]	R^2 [-]	$RMSE$ [m/s, °]	circular offset [°]
40	Standard	99.9	WS	1.028	0.989	0.32	N/A
			WD	1.003	0.999	1.34	0.67
	Adaptive	100.0	WS	1.028	0.989	0.32	N/A
			WD	1.003	0.999	1.33	0.67
106	Standard	99.8	WS	1.000	0.997	0.16	N/A
			WD*	1.001	0.999	0.98	0.24
	Adaptive	99.9	WS	1.000	0.997	0.16	N/A
			WD*	1.001	0.999	0.98	0.24
178	Standard	98.0	WS	0.994	0.996	0.19	N/A
			WD†	0.999	0.999	0.95	-0.20
	Adaptive	98.8	WS	0.994	0.996	0.19	N/A
			WD†	0.999	0.999	0.98	-0.20
244	Standard	92.5	WS	0.995	0.997	0.18	N/A
			WD	0.996	0.998	1.43	-1.00
	Adaptive	95.5	WS	0.995	0.997	0.19	N/A
			WD	0.996	0.998	1.50	-1.01

* Wind direction from the vane was measured at 103 m.

† Wind direction from the vane was measured at 175 m.

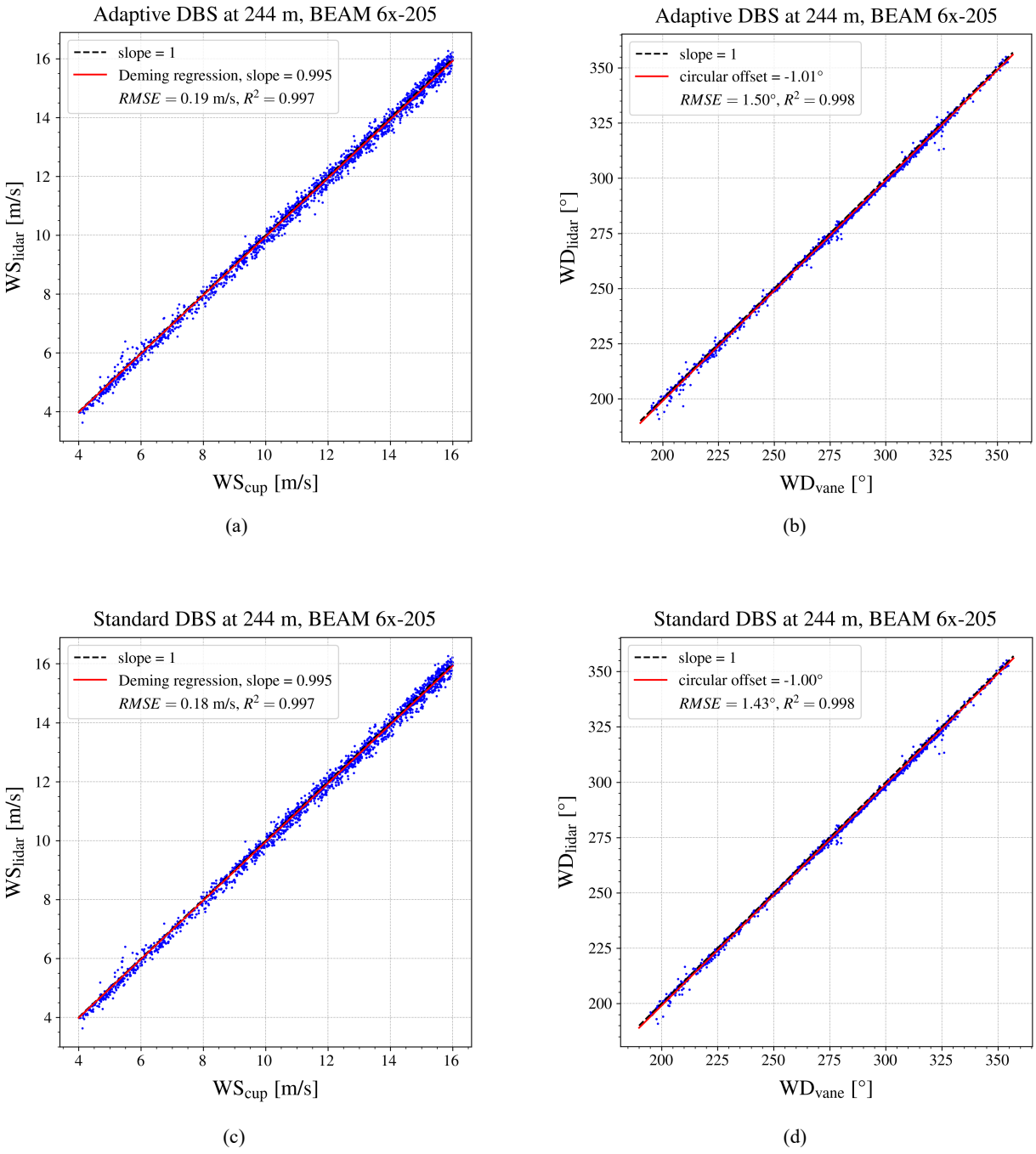

Figure 5. Ten-minute mean wind speeds (a) and wind directions (b) from adaptive DBS applied to Doppler velocities from BEAM 6x-205 profiling lidar, compared with reference measurements from cup anemometers and wind vanes mounted at 244 m on the Light Mast North. Corresponding plots for standard DBS are shown for mean wind speeds (c) and wind directions (d).

Following the validation of the adaptive DBS, availability profiles were computed for all three lidar units. Figure 6a shows the availability of BEAM 6x-205 across ranges from 40 m to 500 m, reported in 10 m increments. For this unit, the availability obtained with the standard and adaptive DBS methods is nearly identical up to approximately 150 m. Beyond this range, the adaptive method provides a consistent improvement, with the difference gradually increasing and reaching a maximum of 15.3 percentage points at 500 m height.

A similar analysis was performed for BEAM 6x-320 (Figure 6b) and 325 (Figure 6c), with availability assessed in 20 m range gates up to 980 m altitude. The results show that the difference in wind velocity availability between the two methods starts from lower altitudes and increases with height. For BEAM 6x-320, the maximum improvement in availability with the adaptive method is observed to be 16.9 percentage points. Similarly, BEAM 6x-325 showed a maximum improvement of 12.9 percentage points. The relative availability differences between two methods are also presented in Figure 6d. As SNR decreases with altitude, the adaptive DBS delivers higher availability, reflecting the benefit of dynamically selecting beam combinations rather than relying exclusively on beams 1 to 5.

Across all three lidars, the adaptive approach consistently achieves availability equal to or greater than that of the standard method. Differences in availability profiles between instruments may be partly attributed to atmospheric variability, since measurements were collected during different time periods. BEAM 6x-320 and 325 show greater similarity, likely due to a one-month overlap in their campaigns. Instrument-specific hardware and optical performance characteristics may also contribute to the observed variability among devices.

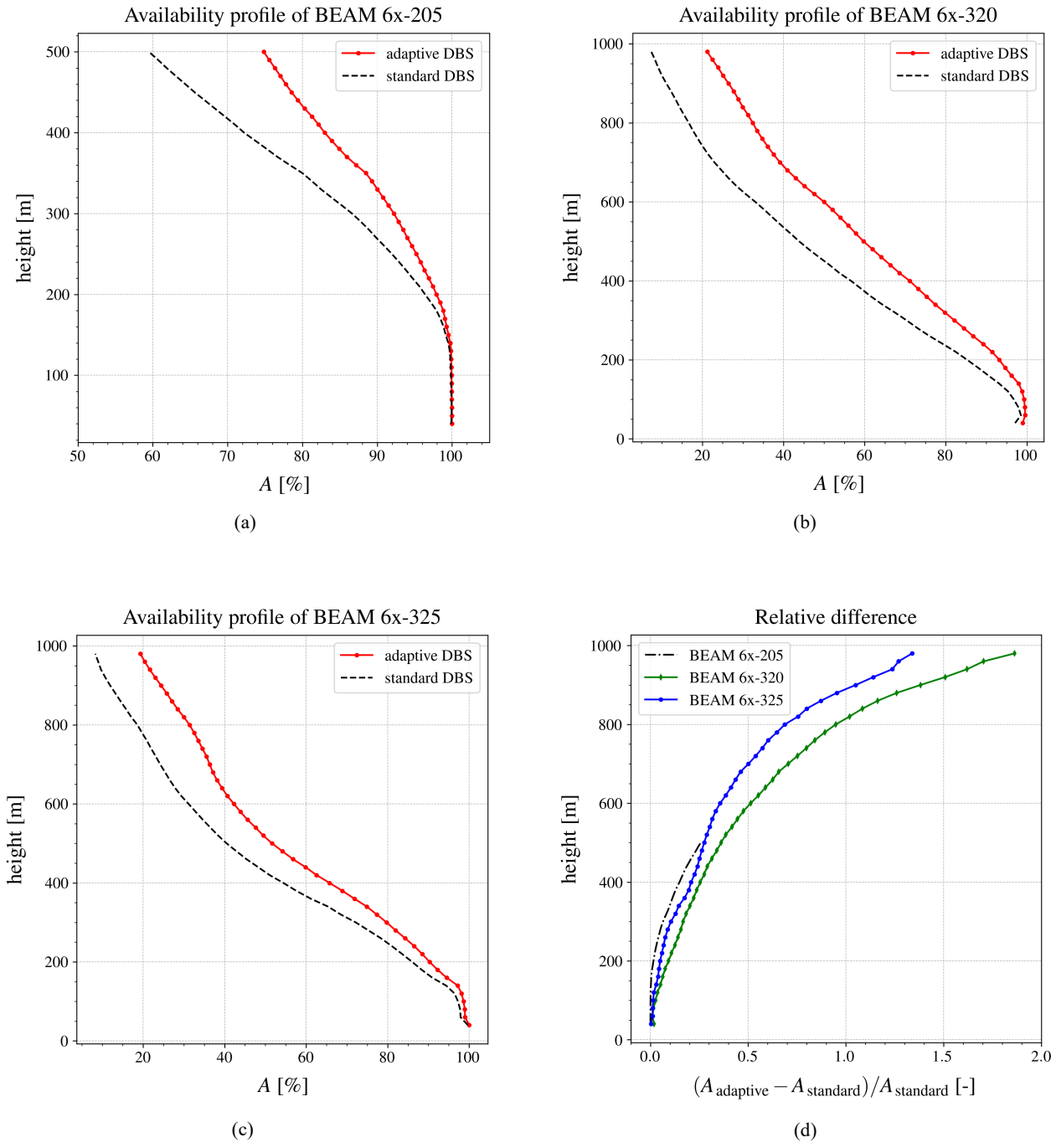

Figure 6. Availability profiles obtained using both adaptive and standard DBS applied to Doppler velocities from BEAM 6x-205 (a), BEAM 6x-320 (b), and BEAM 6x-325 (c). Relative differences between the two methods across the three instruments at various altitudes are also shown (d).

A distribution analysis of the number of beams used for adaptive DBS applied to Doppler velocities of BEAM 6x-320 (Figure 7) highlights the importance of considering three-, four-, and five-beam combinations. Standard DBS availability is indicated by a black arc, representing the fixed configuration of beams 1–5, similar to implementation in the BEAM 6x software. Interestingly, for the first two heights, after the full six-beam combination, the five-beam combinations, including the standard 1–5 set as well as other five-beam arrangements, account for a higher proportion of availability than the other two groups. At 980 m, the contributions from the three-beam and five-beam combinations are equal, and both are slightly lower than those from the four-beam arrangements. This ranking may change depending on atmospheric conditions and the SNR of the backscattered signals.

In this study, we applied a conservative algorithm that discards three-beam combinations with unit vectors under ill conditions. Nevertheless, the difference between the filtered algorithm and the unfiltered version is negligible in terms of both accuracy and availability, as the proportion of excluded configurations is very low. Simple combinations of ill-conditioned beams (e.g., a fixed combination of beams 1, 4, and 6) yield the lowest accuracy among all 42 configurations (not shown). Therefore, if the proportion of such ill-conditioned combinations increases in the adaptive method, the overall accuracy may be slightly reduced.

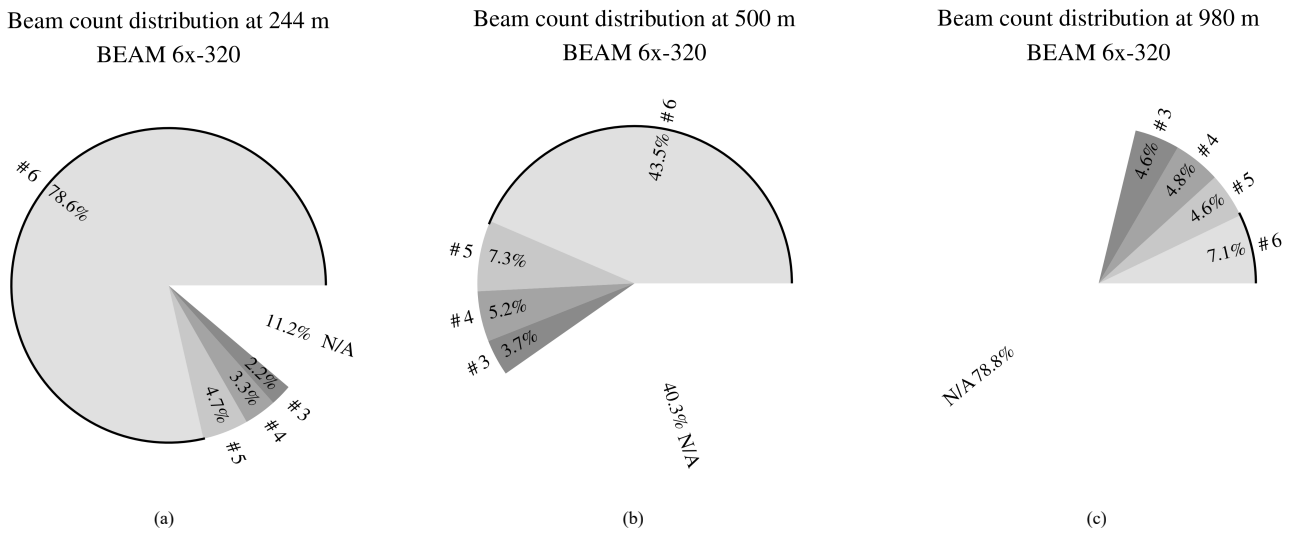

Figure 7. Distribution of beam counts used in adaptive DBS applied to Doppler velocities from BEAM 6x-320 at 244 m (a), 500 m (b), and 980 m (c). The availability of the fixed beam configuration 1–5 is indicated by black arcs, consistent with the implementation in the BEAM 6x software.

5 Conclusion

In this study, a simple method was introduced to enhance the availability of reconstructed wind velocities in pulsed profiling lidars. This approach is an adaptive form of DBS for reconstructing wind velocities, using only beams whose backscattered signals meet the SNR requirement. In contrast to the standard DBS method, which discards an entire scan if the quality of the backscattered signal from a single inclined beam falls below the SNR threshold, the adaptive approach dynamically selects combinations of three to six beams. This maximizes the use of Doppler velocity measurements and increases overall data availability.

The method was validated using three BEAM 6x profiling lidars from Lumibird at the Danish National Test Station for Large Wind Turbines in Østerild, Denmark. The first lidar unit was deployed for nearly three months close to a meteorological mast. After this initial campaign, two additional units were installed at the same site to extend measurements reaching up to 1 km. One unit collected data for two months, the other for one month, with a one-month overlap. Ten-minute averages of wind speed and direction from all three lidars were compared with cup anemometers and wind vanes at four heights on the mast, demonstrating excellent agreement with the reference instruments.

Following this validation, the availability of reconstructed instantaneous wind velocities was compared between the standard and adaptive approaches. The adaptive approach consistently improved availability for all three lidars at higher altitudes. Assessing the availability of two units up to the range gate of 980 m showed that the maximum difference between the two methods is 16.9 percentage points.

Analysis of the beam combinations utilized in the adaptive method for BEAM 6x-320 showed that six-beam combinations dominate, followed by five-, four-, and three-beam combinations. At 980 m, the three- and five-beam contributions are equal and slightly below the four-beam contribution. At this height, the three- and four-beam contributions are of the same order of magnitude as those from the five- and six-beam arrangements, highlighting their role in enhancing availability. Although the validation process revealed no significant difference when removing ill-conditioned three-beam combinations, due to their low occurrence in the algorithm, we opted to exclude them. This precaution ensures that, should their proportion increase in future datasets, accuracy will not be compromised.

Future research could explore these ill-conditioned combinations in more detail to improve understanding of occasional weak estimates. A detailed analysis of the SNR threshold and the necessity of spike filtering is also recommended for future investigations. Moreover, it would be valuable to determine the minimum number of beams required in a profiling lidar to achieve comparable accuracy and data availability.

Appendix A: Validation of DBS methods for the second campaign

Table A1. Validation of DBS methods using Doppler velocities from BEAM 6x-320. Estimated wind speed (WS) and wind direction (WD) are compared with reference cup anemometer and wind vane measurements.

height [m]	method	A [%]	variable	Deming regression, slope [-]	R^2 [-]	$RMSE$ [m/s, °]	circular offset [°]
40	Standard	97.1	WS	1.034	0.979	0.36	N/A
			WD	0.996	0.998	1.80	-1.20
	Adaptive	98.9	WS	1.035	0.977	0.37	N/A
			WD	0.996	0.997	2.18	-1.17
106	Standard	96.5	WS	1.003	0.997	0.16	N/A
			WD*	0.994	0.997	1.90	-1.62
	Adaptive	99.2	WS	1.003	0.997	0.16	N/A
			WD*	0.994	0.997	1.90	-1.61
178	Standard	88.3	WS	0.997	0.998	0.15	N/A
			WD†	0.991	0.995	2.57	-2.34
	Adaptive	94.8	WS	0.997	0.998	0.16	N/A
			WD†	0.991	0.995	2.60	-2.35
244	Standard	78.7	WS	0.995	0.997	0.18	N/A
			WD	0.989	0.993	3.16	-2.93
	Adaptive	88.8	WS	0.995	0.997	0.19	N/A
			WD	0.989	0.993	3.20	-2.92

* Wind direction from the vane was measured at 103 m.

† Wind direction from the vane was measured at 175 m.

Table A2. Validation of DBS methods using Doppler velocities from BEAM 6x-325. Estimated wind speed (WS) and wind direction (WD) are compared with reference cup anemometer and wind vane measurements.

height [m]	method	A [%]	variable	Deming regression, slope [-]	R^2 [-]	$RMSE$ [m/s, °]	circular offset [°]
40	Standard	99.7	WS	1.012	0.987	0.27	N/A
			WD	0.990	0.994	3.11	-2.69
	Adaptive	100.0	WS	1.012	0.987	0.28	N/A
			WD	0.990	0.994	3.11	-2.69
106	Standard	97.1	WS	1.004	0.997	0.16	N/A
			WD*	0.988	0.994	3.31	-3.20
	Adaptive	98.5	WS	1.004	0.997	0.16	N/A
			WD*	0.988	0.994	3.31	-3.21
178	Standard	88.7	WS	0.995	0.996	0.18	N/A
			WD†	0.986	0.991	3.81	-3.73
	Adaptive	92.5	WS	0.995	0.996	0.18	N/A
			WD†	0.986	0.992	3.82	-3.74
244	Standard	80.5	WS	0.995	0.996	0.20	N/A
			WD	0.984	0.988	4.45	-4.36
	Adaptive	86.0	WS	0.995	0.996	0.20	N/A
			WD	0.984	0.988	4.45	-4.36

* Wind direction from the vane was measured at 103 m.

† Wind direction from the vane was measured at 175 m.

Appendix B: Fitting angle versus angle

Let α_i and β_i, $i = 1, ..., N$, be two concurrent estimations of wind directions. How do we find the offset angle γ that makes the two sets of angles match best? We want the unit vectors corresponding to angles $\alpha_i + \gamma$ and β_i to align as well as possible, i.e. we want to maximize the dot product between those vectors. That leads us to define the alignment as

$$A = \sum_{i=1}^{N} \cos(\alpha_i + \gamma - \beta_i), \tag{B1}$$

and seek for the maximum of this quantity. This is obtained by looking for γ's where

$$\frac{dA}{d\gamma} = -\sum_{i=1}^{N} \sin(\alpha_i + \gamma - \beta_i) = 0, \tag{B2}$$

implying

$$\sin\gamma \sum_{i=1}^{N} \cos(\alpha_i - \beta_i) + \cos\gamma \sum_{i=1}^{N} \sin(\alpha_i - \beta_i) = 0. \tag{B3}$$

The extremum is thus

$$\gamma = \arctan\left(\frac{-\sum_{i=1}^{N} \sin(\alpha_i - \beta_i)}{\sum_{i=1}^{N} \cos(\alpha_i - \beta_i)} \right). \tag{B4}$$

The final value is either γ or $\gamma + \pi$, depending on which gives the highest A.

Data availability. Data will be provided upon request, subject to the decision of the Technical University of Denmark and Lumibird SA.

Author contributions. MM: draft, methodology, software, and analysis. GL and JM: conceptualization, methodology, supervision, and funding acquisition. MS: methodology, supervision, analysis, review, and funding acquisition. GG: supervision, review, and funding acquisition.

Competing interests. JM holds a chief editor position in the Wind Energy Science (WES) journal. MM, GL, and GG are employed by Lumibird SA.

Acknowledgements. This project has received funding from the European Union's Horizon Europe research and innovation program under the Marie Skłodowska-Curie grant agreement No 101119550. The authors acknowledge Jesper Grossmann Hansen, Hazal Ozcan, Ginka Georgieva Yankova, Valur Aðalsteinsson Vestmann, Allan Djernes Blaabjerg, and other contributors from the Testing and Calibration (TAC) section of DTU Wind and Energy Systems for performing field experiments and collecting the required datasets. Special thanks to Abdul Haseeb Syed for valuable input and discussion. Contributions from Poul Hummelshøj and Hans-Juergen Kirtzel (METEK Nordic ApS, and METEK GmbH Deutschland) are also acknowledged.

References

Browning, K. A. and Wexler, R.: The Determination of Kinematic Properties of a Wind Field Using Doppler Radar, Journal of Applied Meteorology and Climatology, 7, 105 – 113, https://doi.org/10.1175/1520-0450(1968)007<0105:TDOKPO>2.0.CO;2, 1968.

Ceolato, R. and Berg, M. J.: Aerosol light extinction and backscattering: A review with a lidar perspective, Journal of Quantitative Spectroscopy and Radiative Transfer, 262, 107 492, https://doi.org/https://doi.org/10.1016/j.jqsrt.2020.107492, 2021.

HALO Photonics by Lumibird: BEAM 6x Wind Sciences, https://halo-photonics.com/lidar-systems/beam-6x/, accessed: 2025-09-05, 2024.

Hansen, J. G. and Yankova, G. G.: Calibration of Ground-Based Lidar Beam6X-205, Lc i-243 (en)-r0, DTU Wind Energy, Roskilde, Denmark, 2024.

IEC: Standard IEC 61400-50-1: Wind energy generation systems – Part 50-1: Wind measurement – Application of meteorological mast, nacelle and spinner mounted instruments, 2022.

Lehmann, V. and Brown, W.: Radar Wind Profiler, pp. 901–933, Springer International Publishing, Cham, ISBN 978-3-030-52171-4, https://doi.org/10.1007/978-3-030-52171-4_31, 2021.

Lhermitte, R. M.: Precipitation motion by pulse Doppler, in: Proc. 9th Weather Radar Conf., Amer. Meteor. Soc., pp. 218–223, 1961.

Measures, R.: Laser Remote Sensing: Fundamentals and Applications, Wiley, ISBN 9780471081937, 1984.

Newsom, R. K., Brewer, W. A., Wilczak, J. M., Wolfe, D. E., Oncley, S. P., and Lundquist, J. K.: Validating precision estimates in horizontal wind measurements from a Doppler lidar, Atmospheric Measurement Techniques, 10, 1229–1240, https://doi.org/10.5194/amt-10-1229-2017, 2017.

Peña, A.: Østerild: A natural laboratory for atmospheric turbulence, Journal of Renewable and Sustainable Energy, 11, 063 302, https://doi.org/10.1063/1.5121486, 2019.

Steinheuer, J., Detring, C., Beyrich, F., Löhnert, U., Friederichs, P., and Fiedler, S.: A new scanning scheme and flexible retrieval for mean winds and gusts from Doppler lidar measurements, Atmospheric Measurement Techniques, 15, 3243–3260, https://doi.org/10.5194/amt-15-3243-2022, 2022.

van Dooren, M. F.: Doppler Lidar Inflow Measurements, pp. 717–750, Springer International Publishing, Cham, ISBN 978-3-030-31307-4, https://doi.org/10.1007/978-3-030-31307-4_35, 2022.

van Kuik, G., Peinke, J., Nijssen, R., Lekou, D., Mann, J., Sørensen, J., Ferreira, C., Van Wingerden, J.-W., Schlipf, D., Gebraad, P., Polinder, H., Abrahamsen, A., Van Bussel, G., Sørensen, J., Tavner, P., Bottasso, C., Muskulus, M., Matha, D., Lindeboom, H., Degraer, S., Kramer, O., Lehnhoff, S., Sonnenschein, M., Sørensen, P., Künneke, R., Morthorst, P., and Skytte, K.: Long-term research challenges in wind energy – a research agenda by the European Academy of Wind Energy, Wind Energy Science, 1, 1–39, https://doi.org/10.5194/WES-1-1-2016, 2016.

Veers, P., Dykes, K., Lantz, E., Barth, S., Bottasso, C. L., Carlson, O., Clifton, A., Green, J., Green, P., Holttinen, H., Laird, D., Lehtomäki, V., Lundquist, J. K., Manwell, J., Marquis, M., Meneveau, C., Moriarty, P., Munduate, X., Muskulus, M., Naughton, J., Pao, L., Paquette, J., Peinke, J., Robertson, A., Rodrigo, J. S., Sempreviva, A. M., Smith, J. C., Tuohy, A., and Wiser, R.: Grand challenges in the science of wind energy, Science, 366, eaau2027, https://doi.org/10.1126/science.aau2027, 2019.

Veers, P., Bottasso, C. L., Manuel, L., Naughton, J., Pao, L., Paquette, J., Robertson, A., Robinson, M., Ananthan, S., Barlas, T., Bianchini, A., Bredmose, H., Horcas, S. G., Keller, J., Madsen, H. A., Manwell, J., Moriarty, P., Nolet, S., and Rinker, J.: Grand challenges in the design, manufacture, and operation of future wind turbine systems, Wind Energy Science, 8, 1071–1131, https://doi.org/10.5194/wes-8-1071-2023, 2023.